UDC 621.928:678.7:539.4:620.178.16 DOI: https://doi.org/10.15407/geotm2025.175.101

DETERMINATION OF RUBBER LINING THICKNESS WITH ACCOUNTING DISSIPATIVE LOSSES AND VISCOELASTIC RESPONSE

[1]Kalhankov Ye., [1]Lysytsia M., [2]Kromik A., [1]Ahaltsov H., [1]Novikova A., [3]Tolstenko O.
[1]*M.S. Poliakov Institute of Geotechnical Mechanics of the National Academy of Sciences of Ukraine*
[2]*ALUMATEC GmbH*
[3]*Dnipro State Agrarian and Economic University*

Abstract. The article is devoted to the engineering-based selection of the rubber lining thickness used in ball mills with accounting dissipative losses and the viscoelastic response of the material. It is shown that empirical schemes including DEM models require significant calibration, whereas for design, a concise and physically interpreted methodology is needed at the stage of preliminary selection of the plate thickness. Herein, an approach is proposed in which the energy of the ball impact (equivalent drop height) is balanced by the energy of the rubber plate deformation, and the effect of the finite thickness and near-incompressibility of the rubber is considered through effective stiffness and transverse "splashing" of the layer. The ratios for the maximum local deformation and the performance criterion $\varepsilon=\delta_{max}/t\leq\varepsilon_{all.}$ are derived, which allow a straightforward determination of the minimum required plate thickness for given energy and kinematic conditions of the first stage of grinding (ball diameter 100–125 mm).

For validation of the proposed methodology, experimental tests were performed by dropping a steel ball with a diameter of 100 mm onto rubber specimens of 50–270 mm thickness. The test series revealed a trend of monotonic increase in the diameter of the indentation and contact parameters with increasing drop height, as well as a pronounced thickness effect: under constant load, an increase in t reduces peak pressures by 15–28% and maximum forces by 11–20%, which is consistent with the expected relaxation of the stress state of the surface layer. Regression 3D response surfaces $P_{max}(t,H)$, $p_0(t,H)$ were constructed for interpolation within the experimental range and for mapping of "safe zones" of operation without additional tests.

The practical recommendations are supplemented with constructive conclusions: the trapezoidal "plate-H-wave" configuration rapidly acquires optimal morphometric parameters within the first weeks of operation and contributes to productivity growth by 10–15%, a reduction in the specific consumption of balls by 15–20%, an increase in the yield of the finished product by 3–7% and a decrease in specific energy consumption by 5–10%. The proposed methodology is a reproducible engineering tool for preliminary calculation of thickness with its further refinement for a specific mill, mode and ore type, complementing DEM and empirical approaches and shortening the "design-test-implementation" cycle.

Keywords. mill, lining thickness, dissipation, deformation, durability, rubber lining, modeling, wear.

1. Introduction

Today, elastomers (rubbers) have become fully fledged structural materials in many industries. In the mining and processing industry, rubber is widely used in conveyor belts, rollers and drums, pipelines, vibration isolators and dampers, as well as in protective linings (liners) of chutes of vibrating feeders and mill drums for ore disintegration [1, 2, 3]. It is known that rubber linings, compared to steel ones, reduce noise and vibration levels and are easier to maintain, which improves safety and reduces downtime [1, 2, 3, 4].

The transition to larger aggregate sizes in modern grinding schemes stimulates requirements for lining reliability. Over the past decades, the diameter of industrial mills has increased to 12–13.4 m with a length of 6–11 m, as confirmed both by data from actual installations (for example, the 12.2-meter Cadia Hill mill) and by developments for GMD drives in 44-foot machines [2, 5, 6]. At the first stage of grinding, large-diameter balls (100–125 mm) are used, which determines the impact-abrasive nature of the load on the rubber plate and increases the sensitivity of lining life to its geometry and thickness [7].

Studies show that rubber lining performs not only a protective function, but also improves the mill operation by damping ball impact, reducing noise and optimizing

Received: 19.09.2025 Accepted: 15.12.2025 Available online: 18.12.2025

loading kinematics [1, 2, 3, 5]. At the same time, the issue of engineering-based justification of the plate thickness and profile for specific operating modes (first stage, large balls, high speeds) is not sufficiently addressed in the literature: an empirical approach through a series of operational tests is widespread, which is expensive and time-consuming [8]. Classical models of the "ball-rubber" collision face a number of difficulties: approximation of the dynamic force characteristic, determination of the combined mass, complexity of equations and inevitable approximation of solutions [8]. In parallel, the DEM-based approaches were developed to modeling the charge motion and its interaction with lifter/plates, which have significantly advanced the understanding of how geometry influences trajectories, power and wear. However, these models require calibration and significant computational resources [9, 10].

Considering the above limitations, this study proposes an energy-mechanical approach to selecting the thickness of the rubber plate for impact-abrasive charge at the first stage of grinding.

2. Methods

The aim of the research is to develop a concise methodology that combines the energy balance of the plate deformation under the action of a large-diameter ball, the contribution of dissipative losses in the viscoelastic material, and simple verification procedure at the level of bench or industrial data.

The advantage of the proposed approach lies in minimization of the number of empirical parameters and the reproducibility of engineering calculation for the practical lining design. The developed calculation methodology is intended to supplement the existing DEM and empirical approaches, providing a rapid preliminary estimate of the rational thickness with subsequent refinement for a specific mill.

3. Theoretical part

Let us consider the deformation of a rubber plate by a ball. In this case, we assume that the plate rests on a rigid foundation, the mass of the ball is m, and the ball falls from a certain height h. We also assume that the values h, m, the elastic modulus of the rubber E, Poisson's ratio ν and the permissible relative deformation ε are considered known. In the process of interaction between the ball and the plate, the surface portion of the ball indented into the plate is determined by the angle φ (Fig. 1) (this angle varies starting from the zero value φ_0) at the moment of approaching some maximum value at which the speed of the ball drops to zero.

In the first approximation, it is assumed that ball interacts only with cylindrical part of the plate, marked with dashed lines in Fig. 1. In the process of the ball indentation, the radius of this cylinder increases to a maximum value, which is determined by the angle φ_1, and the stiffness of the cylinder compressed by the ball obviously increases from zero.

To determine the vertical reaction of the cylinder to its deformation, let us extract from it a coaxial cylinder with annular cross-section of area d_s, which corresponds to an elementary increase in the angle φ. In Fig. 1, the axial cross-section of this "elementary" cylinder is shaded and has a radius $R\sin\varphi$. The thickness of its wall can be expressed as $d = R \cdot d\varphi \cdot \cos\varphi$, as shown in Fig. 2.

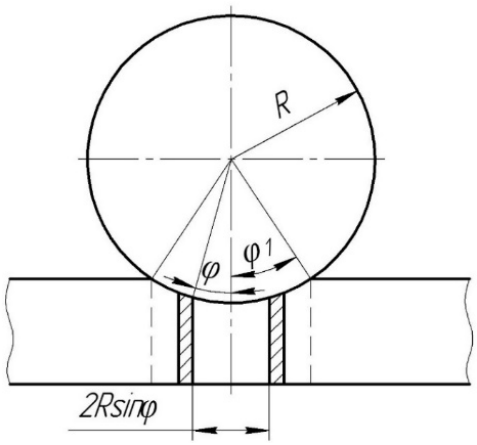

Figure 1 – Scheme of rubber plate

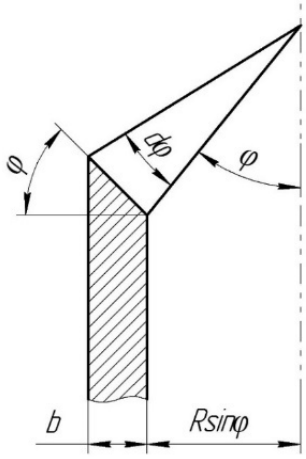

Figure 2 – Calculation scheme deformation

Considering this, the area of the ring is defined as

$$ds = 2 \cdot \pi \cdot R \cdot \sin\varphi \cdot R \cdot d\varphi \cdot \cos\varphi,$$

where R is radius of the ball.

The stiffness coefficient of a rod having such an area is defined accordingly as

$$dC = \frac{E \cdot ds}{l},$$

where l is the thickness of the plate, E is the modulus of elasticity.

Then the axial reaction of dF to vertical deformation Δ is defined as

$$dF = \Delta \cdot dC,$$

where $\Delta = R \cdot \cos\varphi - R \cdot \cos\varphi_1$.

That is

$$dF = R \cdot \left(\cos\varphi - \cos\varphi_1\right) \cdot \frac{2 \cdot \pi \cdot R^2 \cdot E}{l} \cdot \sin\varphi \cdot \cos\varphi \cdot d\varphi$$

Full elastic compression resistance

$$F = \int_0^{\varphi_1} \frac{2 \cdot \pi \cdot R^3 \cdot E}{l} \cdot \left(\cos\varphi - \cos\varphi_1\right) \cdot \cos\varphi \cdot \sin\varphi \cdot d\varphi =$$

$$= \frac{2 \cdot \pi \cdot R^3 \cdot E}{l} \left[\int_0^{\varphi_1} \cos^2\varphi \cdot \sin\varphi \cdot d\varphi - \cos\varphi_1 \cdot \int_0^{\varphi_1} \cos\varphi \cdot \sin\varphi \cdot d\varphi \right] =$$

$$= \frac{2 \cdot \pi \cdot R^3 \cdot E}{l} \left[\left(-\frac{1}{3} \cos^3 \varphi \right) \Big|_0^{\varphi_1} + \cos \varphi_1 \left(\frac{1}{2} \cos^2 \varphi \right) \cdot \Big|_0^{\varphi_1} \right] =$$

$$= \frac{2 \cdot \pi \cdot R^3 \cdot E}{l} \left[\frac{1}{3} - \frac{1}{3} \cos^3 \varphi_1 + \frac{1}{2} \cos^3 \varphi_1 - \frac{1}{2} \cos \varphi_1 \right] =$$

$$= \frac{2 \cdot \pi \cdot R^3 \cdot E}{l} \left[\frac{1}{3} + \frac{1}{6} \cos^3 \varphi_1 - \frac{1}{2} \cos \varphi_1 \right]$$

The work done by this force when the ball is indented into the rubber plate is expressed as

$$A_1 = \int_0^{\varphi} dF\Delta = \frac{2 \cdot \pi \cdot R^4 \cdot E}{l} \int_0^{\varphi_1} \left(\cos \varphi - \cos \varphi_1 \right)^2 \cdot \sin \varphi \cdot \cos \varphi \cdot d\varphi =$$

$$= \frac{2 \cdot \pi \cdot R^4 \cdot E}{l} \int_0^{\varphi_1} \left(\cos^3 \varphi \cdot \sin \varphi - 2 \cdot \cos \varphi_1 \cdot \cos^2 \varphi \cdot \sin \varphi + \cos^2 \varphi_1 \cdot \cos \varphi \cdot \sin \varphi \right) \cdot d\varphi =$$

$$= \frac{2 \cdot \pi \cdot R^4 \cdot E}{l} \left[\left(-\frac{1}{4} \cos^4 \varphi \right) \Big|_0^{\varphi_1} + 2 \cdot \cos \varphi_1 \cdot \left(\frac{1}{3} \cos^3 \varphi_1 \right) \Big|_0^{\varphi_1} - \cos^2 \varphi_1 \cdot \left(\frac{1}{2} \cos^2 \varphi \right) \Big|_0^{\varphi_1} \right] =$$

$$= \frac{2 \cdot \pi \cdot R^4 \cdot E}{l} \left[\frac{1}{4} - \frac{1}{4} \cos^4 \varphi_1 + \frac{2}{3} \cos^4 \varphi_1 - \frac{2}{3} \cos \varphi_1 - \frac{1}{2} \cos^4 \varphi_1 + \frac{1}{2} \cos^2 \varphi_1 \right] =$$

$$= \frac{2 \cdot \pi \cdot R^4 \cdot E}{l} \left[\frac{1}{4} - \frac{1}{12} \cos^4 \varphi_1 + \frac{1}{2} \cos^2 \varphi_1 - \frac{2}{3} \cos \varphi_1 \right]$$

It is quite evident that the portion of the rubber plate volume located outside the cylinder radius $R \cdot \sin \varphi$ will also resist indention and restrict transverse deformation of the cylinder itself. If during compression the radius of the cylinder increases by Δr, then its volume increase can be expressed as

$$\Delta V = \left[(r + \Delta r)^2 - r^2 \right] \cdot l \cdot \pi , \tag{1}$$

The volume of the segment indented into the rubber plate according to Fig. 3 is

$$\Delta V = \pi \cdot h^2 \cdot \left(R - \frac{h}{3} \right),$$

accounting that $h = R - R \cdot \cos \varphi$,

$$\Delta V = \pi \cdot R^2 \left(1 - \cos \varphi \right)^2 \cdot \left(R - \frac{1 - \cos \varphi}{3} R_1 \right) = \pi \cdot R^3 \left(1 - \cos \varphi \right)^2 \cdot \left(1 - \frac{1}{3} + \frac{\cos \varphi}{3} \right) =$$

$$= \pi \cdot R^3 \left(1 - \cos \varphi \right)^2 \cdot \left(\frac{2}{3} + \frac{\cos \varphi}{3} \right). \tag{2}$$

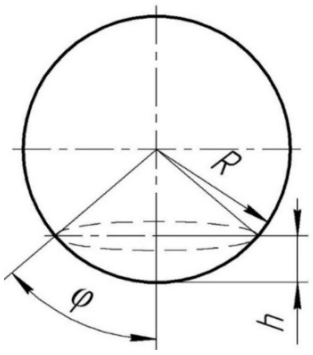

Figure 3 – Scheme for calculating the volume of the indented segment

By equating the volumes determined by formulas (1) and (2) for Δr, we obtain

$$\left(\Delta r^2 + 2r \cdot \Delta r\right) \cdot l \cdot \pi = \pi \cdot R^3 \cdot \left(1 - \cos\varphi\right)^2 \cdot \left(\frac{2}{3} + \frac{\cos\varphi}{3}\right),$$

or

$$\Delta r^2 + 2 \cdot \Delta r \cdot R \cdot \sin\varphi - \frac{R^3}{l} \cdot \left(\left(1 - \cos\varphi\right)^2 \cdot \left(\frac{2}{3} + \frac{\cos\varphi}{3}\right)\right) = 0$$

$$\Delta r^2 + 2 \cdot \Delta r \cdot R \cdot \sin\varphi - \frac{R^3}{3 \cdot l} \cdot \left(1 - 2 \cdot \cos\varphi + \cos^2\varphi\right) \cdot \left(2 + \cos\varphi\right) = 0$$

$$\Delta r^2 + 2 \cdot \Delta r \cdot R \cdot \sin\varphi - \frac{R^3}{3 \cdot l} \cdot \left(2 - 4 \cdot \cos\varphi + 2 \cdot \cos^2\varphi + \cos\varphi - 2 \cdot \cos^2\varphi + \cos^3\varphi\right) = 0$$

$$\Delta r^2 + 2 \cdot \Delta r \cdot R \cdot \sin\varphi - \frac{R^3}{3 \cdot l} \cdot \left(2 - 3 \cdot \cos\varphi + \cos^3\varphi\right) = 0$$

From where

$$\Delta r = -R \cdot \sin\varphi \pm \sqrt{R^2 \cdot \sin^2\varphi + \frac{R^3}{3 \cdot l} \cdot \left(2 - 3 \cdot \cos\varphi + \cos^3\varphi\right)}$$

$$\Delta r = R\left(\sqrt{\sin^2\varphi + \frac{R}{3 \cdot l} \cdot \left(2 - 3 \cdot \cos\varphi + \cos^3\varphi\right)} - \sin\varphi\right) \qquad (5)$$

For a pipe with an inner radius r and an outer radius r_1, under the action of internal pressure *P*, a radial deformation can be obtained [11]

$$\Delta r = \frac{r}{E} \cdot P \cdot \left[\left(\frac{r_1^2 + r^2}{r_1^2 - r^2}\right) + \mu\right],$$

where μ is Poisson's ratio.

It is obvious that for the case when $r_1 \gg r$

$$\Delta r = \frac{r \cdot P}{E} \cdot (1 + \mu). \tag{6}$$

From formula (6), taking into account (5) for pressure P, we obtain

$$p = \frac{E}{R \cdot \sin\varphi \cdot (1 + \mu)} \cdot R\left(\sqrt{\sin^2\varphi + \frac{R}{3 \cdot l}\left(2 - 3 \cdot \cos\varphi + \cos^3\varphi\right)} - \sin\varphi \right).$$

The work of transverse deformation under pressure p is defined as

$$A_2 = \int_0^{\varphi_1} P \cdot 2 \cdot \pi \cdot r \cdot l \cdot dr = \int_0^{\varphi_1} p \cdot 2 \cdot \pi \cdot R \cdot \sin\varphi \cdot l \cdot R \cdot \cos\varphi \cdot d\varphi =$$

$$= \int_0^{\varphi_1} \frac{E \cdot 2 \cdot \pi \cdot l \cdot R^2 \cdot \cos\varphi}{1 + \mu} \cdot \left(\sqrt{\sin^2\varphi + \frac{R}{3 \cdot l} \cdot \left(2 - 3 \cdot \cos\varphi + \cos^3\varphi\right)} - \sin\varphi \right) d\varphi .$$

By equating the energy of a ball with mass m falling from a height h to the energy of deformation of a rubber plate during deceleration, we obtain $m \cdot g \cdot h = A_1 + A_2$

$$m = \frac{4}{3} \cdot \pi \cdot R^3 \cdot \gamma = \frac{4}{3} \cdot 3{,}14 \cdot 0{,}005^3 \cdot 7{,}800 = 4{,}084\,\text{kg},$$

where γ is the density of the metal.

That is

$$mgh = \frac{2\pi R^4 E}{l}\left[\frac{1}{4} - \frac{1}{12}\cos^4\varphi_1 + \frac{1}{2}\cos^2\varphi_1 - \frac{2}{3}\cos\varphi_1 \right] + \frac{2\pi R^2 El}{1 + \mu} \int_0^{\varphi_1} f(\varphi) \cdot d\varphi$$

$$f(\varphi_1) = \cos\varphi \left[\sqrt{\sin^2\varphi + \frac{R}{3 \cdot l}\left(2 - 3\cos\varphi + \cos^3\varphi\right)} - \sin\varphi \right]. \tag{7}$$

Given that height value h is known, formula (7) makes it possible to find the angle that determines the maximum compression deformation of the rubber plate Δl:

$$\Delta l = R - R\cos\varphi_1 . \tag{8}$$

For a numerical example, the input data are taken for the rubber lining of the ore grinding ball mill with a diameter of 4.5 m, in which a metal ball with diameter $d = 0{,}1\,\text{m}$ and mass of 4.084 kg falls on a plate with a thickness of $l = 0{,}27\,\text{m}$. The lining is made of highly filled rubber of grade A, which has 65 parts by mass of technical carbon and features the following mechanical characteristics: modulus of elasticity E = 8 MPa; Poisson's ratio ν = 0.495; density ρ = 1150 kg/m³; ultimate tensile

stress σ = 15 MPa; allowable relative deformation ε_{all} = 0.35; energy dissipation coefficient ψ = 0.6.

Dividing the angular deformation φ_1 into 5 parts and using the trapezoidal formula [12], we obtain

$$m \cdot g \cdot h = \frac{2 \cdot \pi \cdot R^4 \cdot E}{l}\left[\left(\frac{1}{4} - \frac{1}{12}\cos^4\varphi_1 + \frac{1}{2}\cos^2\varphi_1 - \frac{2}{3}\cos\varphi_1\right) + \right.$$
$$\left. + \frac{\varphi_1}{5}\left(f\left(\frac{\varphi_1}{5}\right) + f\left(\frac{2\cdot\varphi_1}{5}\right) + f\left(\frac{3\cdot\varphi_1}{5}\right) + f\left(\frac{4\cdot\varphi_1}{5}\right) + \frac{1}{2}f\left(\varphi_1\right)\right) \cdot \frac{l^2}{R^2 \cdot (1+\mu)}\right] \quad (9)$$

The graphical solution of equation (9), constructed by the Microsoft Excel processor, is shown in Fig. 4, in which the left side of equation (9) is denoted by y_1 and its right side – by y_2.

As follows from Fig. 4, $\varphi_1 = 1{,}05$ rad and in this case the deformation energy is 178.28 J. For the lining deformation according to formula (8) we obtain $\Delta l = 0.05 - 0.05\cos\varphi_1 = 0.02588$.

Thus, the relative deformation equals:

$$\varepsilon = \frac{\Delta l}{l} = \frac{0.02588}{0{,}27} = 0.09585 \approx 0.1,$$

which, in turn, does not exceed the permissible value of 0.3…0.35.

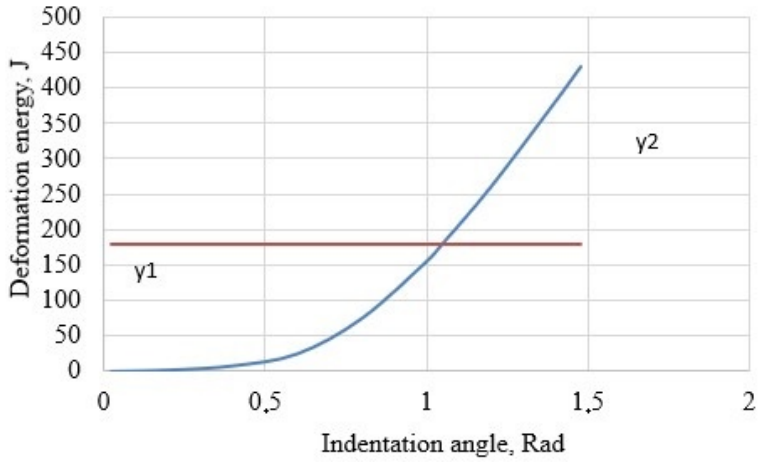

Figure 4 – Scheme for determining deformation

4. Results and discussion

Experimental study of the lining resistance to the impact-indentation action of balls. During the study, the resistance of rubber linings with different thicknesses H to the impact of a steel ball with a diameter of D_b = 100 mm should be evaluated. The main parameters are: the diameter of the indentation D, the depth of the indentation ζ,

the impact-resistance coefficient $Y_g = A / \zeta$, J/mm, (where $A = mgh$), contact values of a, p_0, P_{max} and relative deformation $\varepsilon = \zeta / t$.

A modernized drop-weight hook was used as an experimental installation - its structure and principle of operation are described in detail in reference [13]. The methodology for conducting experimental studies was as follows: steel balls were smeared with chalk and dropped from a given height onto a previously prepared rubber specimen. The rubber specimens, of 150×150 mm size, were prepared from a new lining plate. To simulate the wear process, five standard specimens with sizes of 270 mm, 200 mm, 150 mm, 100 mm and 50 mm were prepared. Then the ball was dropped, and the diameter of the indentation was measured using a vernier caliper; the experiments were repeated 3 times and afterwards, the average size of the indentation was determined, based on which the indentation force and pressure on the lining were calculated.

The results of the experimental studies are shown in Figures 5, 6, 7.

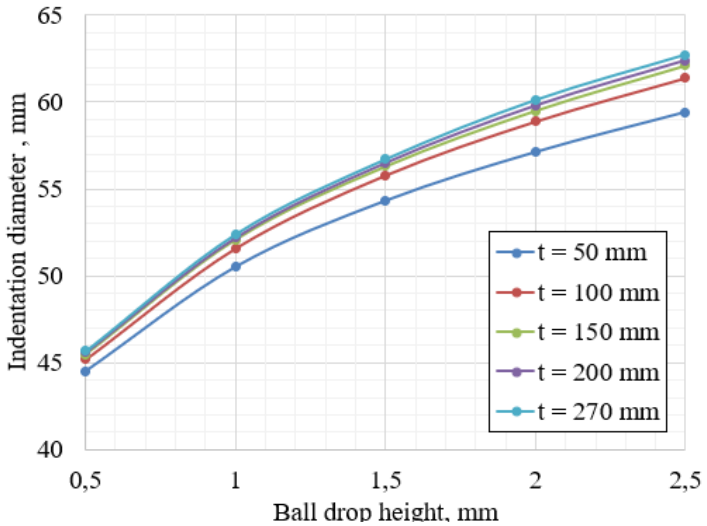

Figure 5 – Dependence of the indentation diameter on the ball drop height for different lining plate thicknesses

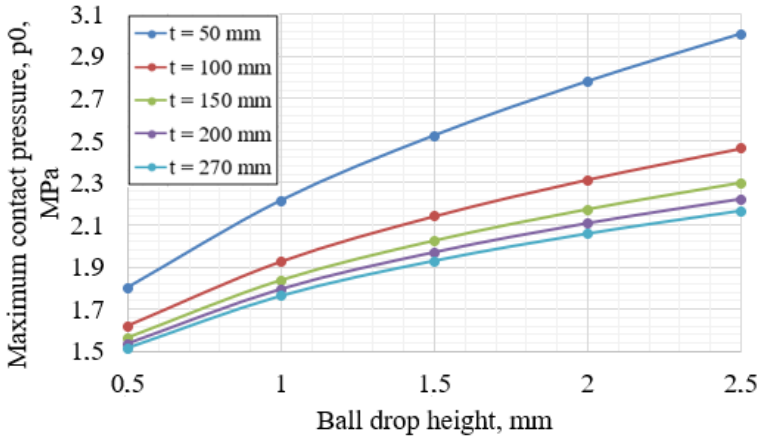

Figure 6 – Dependence of maximum contact pressure on the ball drop height for different thicknesses of the lining plate

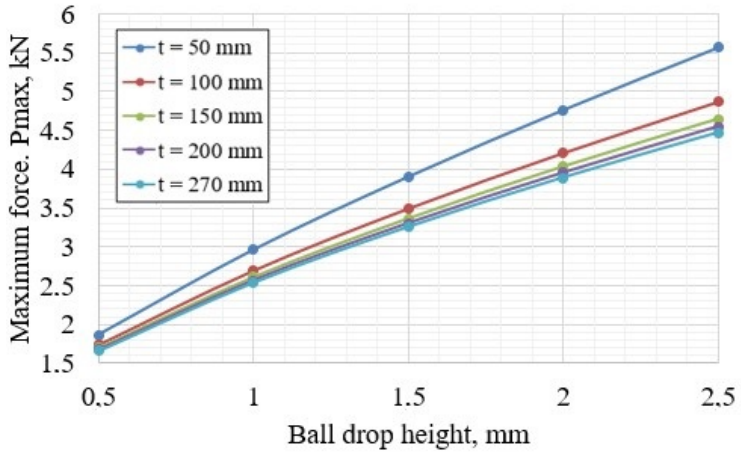

Figure 7 – Dependence of maximum force on the height of the ball drop for different thicknesses of the lining plate

Analysis of the obtained dependence shows a clear monotonic trend: with increasing ball drop height H, the indentation diameter increases for all thicknesses (t). The influence of thickness is evident in the relative position of the curves: a larger t slightly "smears" the contact (the curves lie higher for small H and have a slightly lower steepness at large H), which indicates an increase in the contact area and softening of peak stresses.

Comparison with the indentation diameter shows: with increasing H, the contact pressure rises more intensively than the indentation diameter itself (on average by ~51% when changing H: 0.5 m →2.5 m), while an increase in the thickness t (50 mm →270 mm) reduces peak pressures by 15–28% depending on H. This is a direct indicator of the stress state weakening in the rubber surface layer and the expected increase in fatigue life.

According to Figure 7, the dominance of the impact energy manifests itself particularly clearly: on average, P_{max} increases by approximately +179% when changing H: 0.5 m →2.5 m (≈ 2.8 times). At the same time, increasing the lining thickness from 50 mm to 270 mm at constant H reduces P_{max} by 11–20%, which additionally confirms the damping effect of the thicker plate. Thus, the relationship "$D_{ind,} \rightarrow p_0 \rightarrow P_{max}$" consistently transforms the observed contact geometry into physically meaningful stress-force parameters.

In order to integrate the entire dataset and enable interpolation within the experimental range of parameters, approximation-based 3D visualizations were constructed (Figure 8). Each surface represents a smoothed function of two factors (t, H), obtained by a regression approximation with quadratic terms and by the interaction t-H.

The practical value of such visualization includes three main points:

1. Interpolation without repeated experiments. For any (t, H) within the experimental range, it is possible to rapidly estimate $D_{ind.}$, p_0 or P_{max}. This is useful for analysis, mode selection and preliminary design.

2. Mapping of "safe zones". Projection of the surface in the form of contours (isolines) enables rapid finding those parameter regions where p_0 or P_{max} do not exceed the limit values dictated by the strength or durability criteria. For example, shifting

along the *t* axis at a fixed *H* shows by how many millimeters the plate should be increased to reduce pressure below the target level.

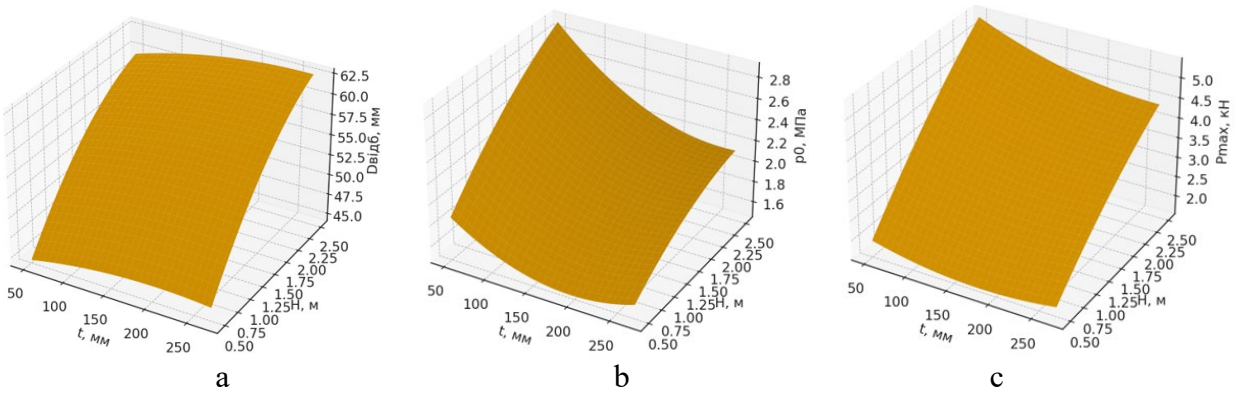

Figure 8 – Approximation-based 3D visualizations for obtaining analytical dependence of the maximum force P_{max} (kN) on the specimen thickness *t* (mm) and the ball drop height *H* (m)

3. Assessment of sensitivity and interaction of factors. The slope of the surface along the *H* and *t* axes indicates which factor is "stronger" at a given point (*t, H*). The curvature (concavity) of the surface reflects the decreasing extensions with increasing factor (saturation effect), while non-uniform gradients show areas where the *t*-*H* interaction strengthens or weakens the response (that is why, for example, increasing thickness gives a greater extension at larger *H*).

Based on the study results, a generalized response field of the lining was formed. This response field is convenient for technical decision-making: from selecting a rational thickness for a given level of ball impact to constructing maps of operational parameters that minimize peak stresses and increase durability.

The analysis of research in the field of lining design and the own industrial studies of the operation of rubber linings also indicate that the most successful lining design is the "Plate-H-Wave" type, i.e., a trapezoidal scalene plate, which, when interacting with the mill charge, attains optimal morphometric parameters within the first weeks of operation and contributes to the reduction of such indicators as energy and balls consumption [14].

The selection of optimal parameters of the rubber lining makes it possible to intensify ore disintegration and significantly improve the key parameters of the grinding process, namely, in this study, the feed rate productivity increased by 10...15%; the specific ball consumption decreased by 15...20%; the yield of the finished product increased by 3...7%; the specific electric energy consumption decreased by 5...10%.

5. Conclusions

A concise and engineer-friendly approach is proposed enabling rapid selection of rubber plate thickness based on the ball impact energy with taking into account the viscoelasticity of rubber and the finite thickness effect. The derived formula calculates the maximum deformation and further enables just a simple check of operability. For example, for a 100 mm ball (mass 4.084 kg) and a 270 mm plate, $\varepsilon = 0.026$–0.050 was obtained, which is significantly below the practical allowable limit of

0.30–0.35; the calculated forces and pressures are within safe limits for the first stage of grinding.

Thus, the starting plate thickness when using 100–125 mm balls can be taken at the level of $t \approx 0.22–0.27$ m with its further verification by the formula with correction for the specific mill mode and rubber properties. Reducing the h_{ef} by kinematics, lining and rubber quality control (dissipation, adhesion) directly improves the service life. The methodology is simple to apply, reduces the number of expensive test runs and helps consistently maintain productivity and energy consumption at the best level.

Conflict of interest

Authors state no conflict of interest.

REFERENCES

1. Eriksson, M. and Furtenbach, L. (2023), "*Stretching the life of your mill liners",* available at: https://www.metso.com/insights/blog/mining-and-metals/stretching-the-life-of-your-mill-liners/ (Accessed 01 July 2025)

2 Dyrda, V., Zozulia, R., Golovko, L., Stoyko, O., Khmil, I. and Kalgankov, E. (2018), *Rezinovyye futerovki rudoizmelchitelnykh melnits ekstremalnykh usloviyakh* [Rubber linings for ore grinding mills in extreme conditions], Zhurnfond, Dnipro, Ukraine.

3. Weir Minerals (2021), *Vulco® mill lining systems,* available at: https://www.global.weir/globalassets/resources/product-pdfs/vulco/vulco-mill-lining-systems-brochure-compressed.pdf (Accessed 01 July 2025)

4. Metso (2025), *Rubber mill liners* [Online], retrieved from: https://www.metso.com/products-and-services/parts/mill-liners/rubber-mill-liners/ (Accessed 01 July 2025)

5. Boughey, A., Svalbonas, V., and Jones, S. (2000), *Supply, installation & commissioning of the world's largest grinding mill*, available at: https://www.boughey.com/Resources/SME2000.pdf (Accessed 01 July 2025)

6. Kalhankov, Y. V. (2020), "Some issues of resource and energy saving in crushing of mineral raw materials in drum ball mills", *Geo-Technical Mechanics*, vol. 151, pp. 138–149. https://doi.org/10.15407/geotm2020.151.138

7. Kalgankov, E., (2017), "Features of fractal analysis of the fracture surface of rubber linings operating under conditions of abrasive fatigue wear", *Geotechnical Mechanics: Interdepartmental Collection of Scientific Papers,* issue 133, available at: https://nasplib.isofts.kiev.ua/handle/123456789/138716 (Accessed 01 July 2025)

8. Weir Minerals (2018), *Vulco® R67 Rubber–Mill Liners,* available at: https://www.global.weir/globalassets/resources/product-pdfs/vulco/vulco-mill-liners-r67-rubber-spec-sheet.pdf (Accessed 01 July 2025)

9. Kalhankov, Y., Lysytsia, M., Ahaltsov, H., Novikova, A. and Lysytsia, N. (2024), "Dynamics of the interaction between the charge and the protective lining inside the drum ball mills", *Geo-Technical Mechanics*, vol. 170, pp. 65–77. https://doi.org/10.15407/geotm2024.170.065

10. Cleary, P. W. (2001), "Charge behaviour and power consumption in ball mills: Sensitivity to mill operating conditions, liner geometry and charge composition", *International Journal of Mineral Processing,* vol. 63, pp. 79–114. https://doi.org/10.1016/S0301-7516(01)00037-0

11. Pysarenko, G.S., Kvitka, O.L. and Umansky, E.S. (2004), *Opir materialiv. Pidruchnyk* [Strength of Materials], 2nd ed., Vyshcha shkola, Kyiv, Ukraine available at: https://btpm.nmu.org.ua/ua/download/Писаренко%20Г.С.%20Опір%20матеріалів.pdf (Accessed 01 July 2025)

12. Kaw, A.K. (2023), LibreTexts. Mathematicsб *7.02: Trapezoidal Rule of Integration*, available at: https://math.libretexts.org/Workbench/Numerical_Methods_with_Applications_(Kaw)/7%3A_Integration/7.02%3A_Trapezoidal_Rule_of_Integration (Accessed 01 July 2025)

13. Dyrda, V., Kalgankov, E., Tsaniidi, I., Chernyi, O. and Pugach, A. (2014), *Prystriy dlya vyprobuvan humovykh elementiv na udar* [Device for testing rubber linings for impact], State Register of Patent of Ukraine, Kyiv, UA, Pat. No. 93011. https://sis.nipo.gov.ua/uk/search/detail/629360/

14. Dyrda, V., Kalashnikov, V., Golovko, L., Kalgankov, E., Khmel, I., Stoyko, O. and Tsaniidi, I. (2016), *Futerivka barabannoho mlyna* [Drum mill lining], State Register of Patent of Ukraine, Kyiv, UA, Pat. No. 105550. https://sis.nipo.gov.ua/uk/search/detail/844119/

About the authors

Kalhankov Yevhen, Engineer in Department of Elastomeric Component Mechanics in Mining Machines, M.S. Poliakov Institute of Geotechnical Mechanics of the National Academy of Sciences of Ukraine, Dnipro, Ukraine, kalhankov.ye.v@dsau.dp.ua, ORCID ***0000-0002-4759-6687***

Lysytsia Mykola, Candidate of Technical Sciences (Ph.D), Senior Researcher, Senior Researcher in Department of Elastomeric Component Mechanics in Mining Machines, M.S. Poliakov Institute of Geotechnical Mechanics of the National Academy of Sciences of Ukraine, Dnipro, Ukraine, vita.igtm@gmail.com ***(Corresponding author)***, ORCID ***0000-0001-6364-8937***

Kromik Andreas, Chief Designer at ALUMATEC GmbH, Kaarst, Germany, info@alumatec.de

Ahaltsov Hennadii, Master of Science, Junior Researcher of Department of Elastomeric Component Mechanics in Mining Machines, M.S. Poliakov Institute of Geotechnical Mechanics of the National Academy of Sciences of Ukraine, Dnipro, Ukraine, ag.gena@gmail.com, ORCID ***0000-0001-6296-7573***

Novikova Alina, Master of Science, Junior Researcher of Department of Elastomeric Component Mechanics in Mining Machines, M.S. Poliakov Institute of Geotechnical Mechanics of the National Academy of Sciences of Ukraine, Dnipro, Ukraine, alina.goncharenko@gmail.com, ORCID ***0000-0002-4861-0196***

Tolstenko Oleksandr, Candidate of Technical Sciences (Ph.D), Associate Professor of the Department of Engineering of Technical Systems, Dnipro State Agrarian and Economic University, Dnipro, Ukraine, tolstenko.o.v@dsau.dp.ua, ORCID ***0000-0003-4752-5704***

ВИЗНАЧЕННЯ ТОВЩИНИ ГУМОВОЇ ФУТЕРОВКИ З УРАХУВАННЯМ ДИСИПАТИВНИХ ВТРАТ ТА ПРУЖНО-В'ЯЗКОЇ ВІДПОВІДІ

Калганков Є., Лисиця М., Кромік А., Агальцов Г., Новікова А.

Анотація. Стаття присвячена інженерно обґрунтованому вибору товщини гумової футеровки кульових млинів із урахуванням дисипативних втрат та пружно-в'язкої відповіді матеріалу. Показано, що емпіричні схеми і навіть DEM-моделі потребують значного калібрування, тоді як для проектування на етапі попереднього вибору необхідна компактна фізично інтерпретована методика. Запропоновано підхід, у якому енергія удару кулі (еквівалентна висота падіння) урівноважується енергією деформації гумової плити, а вплив скінченної товщини та майже некопресибельності гуми враховано через ефективну жорсткість і поперечне «розплескування» шару. Отримано співвідношення для максимальної локальної деформації та критерій працездатності $\varepsilon=\delta_{max}/t\leq\varepsilon_{доп}$, що дозволяє прямолінійно визначати мінімально необхідну товщину плити під задані енергетичні та кінематичні умови першої стадії подрібнення (кулі 100–125 мм).

Для валідації виконано експериментальні випробування ударним падінням сталевої кулі діаметром 100 мм на гумові зразки товщиною 50–270 мм. За результатами серій спостережено монотонне зростання діаметра відбитка та контактних параметрів зі збільшенням висоти скидання, а також виразний товщинний ефект: за сталого навантаження збільшення t знижує пікові тиски на 15–28 % і максимальні сили на 11–20 %, що узгоджується з очікуваним послабленням напруженого стану поверхневого шару. Побудовано регресійні 3D-поверхні відгуку $P_{max}(t,H)$, $p_0(t,H)$ для інтерполяції в дослідному діапазоні та картографування «безпечних зон» експлуатації без додаткових випробувань. Практичні рекомендації доповнено конструктивними висновками: трапецоїдна «плита-H-хвиля» швидко набуває оптимальних морфометричних параметрів у перші тижні роботи та сприяє підвищенню продуктивності на 10–15 %, зниженню питомої витрати куль на 15–20 %, приросту виходу готового продукту на 3–7 % і зменшенню питомої енергоємності на 5–10 %. Запропонована методика є відтворюваним інженерним інструментом попереднього розрахунку товщини з подальшим уточненням під конкретний млин, режим і руду, доповнюючи DEM-та емпіричні підходи та скорочуючи цикл «проектування-випробування-впровадження».

Ключові слова. млин, товщина футеровки, дисипація, деформація, довговічність, гумова футеровка, моделювання, знос.